Received May 18, 2022, accepted June 6, 2022, date of publication June 14, 2022, date of current version June 20, 2022.

Digital Object Identifier 10.1109/ACCESS.2022.3183097

A New Detection Method of the Surface Broken Wires of the Steel Wire Rope Using an Eddy Current Differential Probe

KOU YANFEI[1,2], GUO JIUJIANG[1], LI JINGJING[1], JIAO SHAONI[3], LIU JIQUAN[2], YAN ZHIWEI[2,4], AND ZHU KUN[5]

[1]School of Mechanical Engineering, North University of China, Taiyuan 030051, China
[2]Tai Yuan Research Institute of China Coal Technology & Engineering Group, Taiyuan 030006, China
[3]College of Mechanical and Vehicle Engineering, Taiyuan University of Technology, Taiyuan 030024, China
[4]National Engineering Laboratory for Coal Ming Machinery, Taiyuan 030006, China
[5]China Coal Technology & Engineering Group, Beijing 100013, China

Corresponding author: Kou Yanfei (kouyanfei@163.com)

This work was supported in part by the Science and Technology Program of Shaanxi Administration for Market Regulation under Grant 2019KY06, in part by the Shanxi Science and Technology Department under Grant 201901D211210, in part by the Shanxi Administration for Market Regulation under Grant 20210302124354, in part by the Science and Technology Program of State Administration for Market Regulation under Grant 2020MK103, and in part by the Scientific Research Project of Shanxi Tiandi Coal Machinery Equipment Company Ltd., under Grant M2021-MS11.

ABSTRACT This paper describes a new detection method of the surface broken wires of the steel wire rope based on the conducting property of the rope. The surface of the steel wire rope is spiral. This spiral characteristic has influence on the eddy current (EC) response signal of the broken wires. Therefore, an EC differential probe is designed to improve the detection accuracy. First, a finite element analysis (FEA) of detecting the broken wires with the EC differential probe is conducted. When the probe scans above the intact part of the steel wire rope, the distribution of the EC in the rope just under the probe is symmetrical about the axis of the rope. Then the output voltage of the differential probe is almost zero. Accordingly, the output voltage is out of balance when the surface broken wires appear. The simulation results show that the effect of the surface alternating peaks and valleys of the rope on the EC response signal of the broken wires can be eliminated by the proposed EC differential probe. Then an experimental platform is built to carry out the scanning detection of different degrees of the surface broken wires. It can be observed that when the probe moves above the broken wires, the output voltage of the differential probe is significantly larger. Finally, the obtained scanning signal is post processed using the wavelet-based denoising method to improve the signal-to-noise rate. The experimental results show that the proposed method can effectively identify the damage degrees of the surface broken steel wires.

INDEX TERMS Eddy current differential probe, steel wire rope, surface broken wires, finite element analysis.

I. INTRODUCTION

The steel wire rope is a tensile and load-bearing component, which has been widely used in various major industries such as the agriculture and service industries [1]–[3]. The steel wire rope has a series of advantages, such as light weight, high tensile strength and fatigue strength, good flexibility and working stability, and low winding noise during the high-speed operation [4], [5]. Generally, the steel wire rope is used in relatively harsh operation conditions. Its long-term operation in the air makes it difficult to avoid defects, such as the surface broken wires. The defects pose a serious threat to the safe use of the steel wire rope. According to the statistics from the recent years, accidents caused by the rope breakage are the most cases of the accidents in the lifting equipment. The broken wires are the main cause of the rope breakage accidents. Therefore, the application of the broken wires detection with high precision and high reliability methods is of great significance for improving the safety performance of the steel wire rope [6], [7].

The associate editor coordinating the review of this manuscript and approving it for publication was Xiaokang Yin.

The magnetic flux leakage (MFL) method has been widely applied to the detection of the broken wires. The domestic and foreign scholars also have carried out a lot of researches on its practical applications. Zawada develops a set of MD 120B recording instrument for the steel wire rope based on MFL. The results show that it can be used to predict the decommissioning time of steel wire rope and to detect defects, such as steel fracture and corrosion [8]. Collini uses a portable MFL tester to perform the on-site inspection of cable. The scanning results show that the broken wires caused by wear and fatigue can be detected effectively [9]. Intron Plus also detects the internal and external broken wires of the steel wire rope by the MFL method. The weight of the magnetic head becomes larger as the diameter of the steel wire rope increases [10]. Since the 1980s, Yang has conducted the long-term research on the strong magnetic detection of the steel wire ropes. He uses the permanent magnets to excite the steel wire rope and the Hall elements to measure the MFL around the defect. The quantitative detection of wire breakage defects is achieved [11].

With the development of the non-destructive testing technology, the acoustic emission testing (AET), the ultrasonic testing (UT), the eddy current testing (ECT), and other technologies have also been applied in the detection of broken wire ropes. Quan tests the wire rope of the elevator during the stretching process using AET. The amplitude and energy of the acoustic signal are large when the rope breaks [12]. Raišutis analyzes the propagation of the ultrasonic signal in the steel wire rope using the finite element method and the broken wires is defected [13]. Peng uses the ray method to detect the outer plastic-coated wire rope. The shape of the internal broken wire is more clearly seen compared with the electromagnetic test results [4].

It can be seen that the above researches on the non-destructive testing of the steel wire rope at home and abroad have achieved fruitful results. However, there are still some shortcomings in the practical applications. For instance, the conventional manual visual hanging method is only suitable for the detection of the broken out outward diffusion. It is high labor intensity and low detection efficiency. AET is mainly used for the detection of the continuous media, but not for the non-continuous steel wire rope. UT requires a coupling agent. It increases the difficulty of detecting defects on the surface of the rope and complicates the detection signal. The radiation detection technique needs the special protective radiation measures. MFL needs the object to be magnetized, which has various disadvantages such as uneven saturation magnetization of the steel wire rope, weak anti-interference ability of the sensor, and difficulty in realizing online detection of the wire rope. Fortunately, ECT of the wire rope can avoid the above problems effectively [14]–[17]. Hill models the wire rope with an internal flaw as an infinite conducting circular cylinder. The 3D simulation of the electromagnetic field in the cylinder shows that 10 Hz is a good choice for the detection. But the spiral surface of the rope is not considered during simulation [14]. Hiruma analyses the proximity effect and skin effect in Litz wires and wire rope by the integral method. The distribution of eddy current in the cross section of the rope is symmetrical about the axis of the rope[15]. Cao designs a low frequency eddy current probe for evaluating the broken wires. The probe is symmetrically arranged on the adjustable ring in the radial direction. The identification feature quantity of the broken wires is the voltage amplitude difference and the phase difference between the probe response signal and the excitation signal [16]. Sukhorukov presents a device for detecting broken rope in the conveyor belts by ECT. The local fault and the loss of the metallic area are detected by the eddy current probe with light weight [17].

The ECT of the steel wire rope has market application, but the detection method is still needed to be studied. During the detection of the spiral rope by ECT, the alternating characteristic of the peaks and the valleys of the rope surface affects the detection of the broken wires. In this study, an eddy current (EC) differential probe is designed for the detection of the surface broken wires. In the following contents, the EC probe is described in detail firstly. Then the finite element analyse of detection of the surface broken wires with different degrees is conducted. At last, the eddy current scanning experimental platform is established.

II. DESIGN OF THE EDDY CURRENT DIFFERENTIAL PROBE

A. STRUCTURAL CHARACTERISTIC OF THE STEEL WIRE ROPE

The steel wire rope is made of high carbon steel wire. According to the standards a certain number of rope strands are wound around the rope core. The schematic diagram of a 6×19 ordinary lay wire rope is shown in Fig.1. The axis of the wire rope is parallel to the Z axis. Fig.1 (a) is a front view of the steel wire rope. Fig.1 (b) is a sectional view of the wire rope structure. The alternating peaks and valleys on the surface of the wire rope is shown obviously. Strands 1 and 4, strands 2 and 5, and strands 3 and 6 in Fig.1 (b) are symmetric about the coordinate origin O, respectively.

In [18] the influence of the spiral surface on the EC signal was analyzed. Due to the change of the lift-off between the bottom of coil and the rope surface during the scanning detection, the output voltage varies sinusoidally. Therefore, the influence of the spiral structure on the EC signal induced by the broken wires should be considered. Based on this symmetrical feature, an EC array differential probe was designed in this study to realize the detection of broken wires.

B. DESIGN PRINCIPLE OF THE PROBE

Fig.2 shows the schematic diagram of the EC differential probe designed in this study. The coils a_1 and a_2, b_1 and b_2, and c_1 and c_2 in Fig.2 (a) are placed symmetrically with respect to the origin O. The lift-off is identical to each other. A pair of symmetrically placed coils are differentially connected and the detection signal is the output voltage of the differential bridge. In order to illustrate the detection method, the pair of coils a_1 and a_2 scanning from position 1

to position 2 is shown in Fig.2 (b). The broken wires appear on the surface of the steel wire rope.

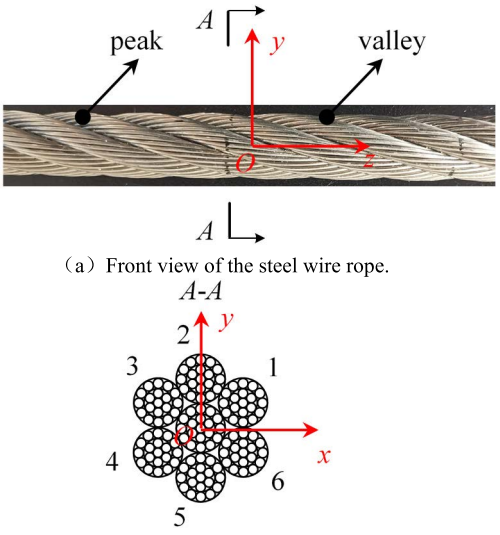

（a）Front view of the steel wire rope.

（b）Sectional view of the steel wire rope.

FIGURE 1. The schematic diagram of a 6 × 19 ordinary lay wire rope.

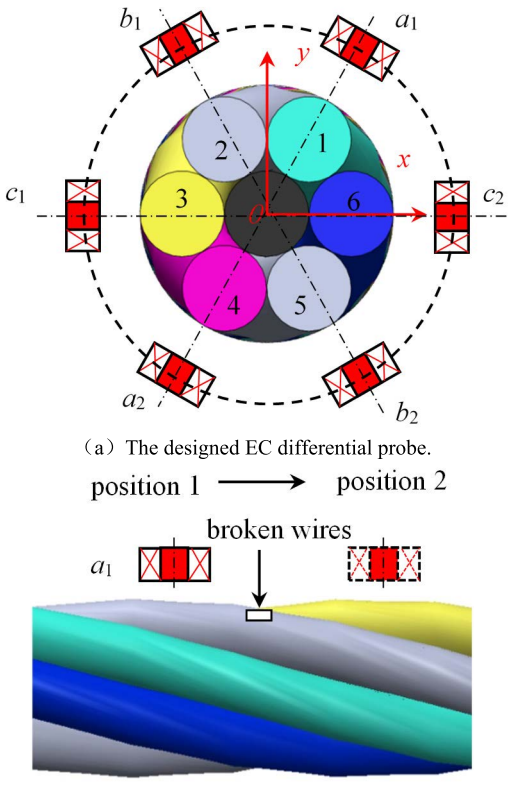

（a）The designed EC differential probe.

（b）Scanning detection of the surface broken wires.

FIGURE 2. The schematic diagram of the EC differential probe with the steel wire rope.

When the EC differential probe scans over the intact part of the surface, the surface of the steel wire rope below the pair of coils that are with the phase difference of 180° is symmetrical. EC on the surface of the steel wire rope is also symmetrical. Thereby the output voltage of the differential bridge in Fig. 2 (a) is zero. EC near the broken wires in Fig. 2 (b) is disturbed. Hence the output voltage of the differential bridge above the broken wires is no longer zero. By analyzing the voltage of the three differential bridge, it is possible to detect the surface broken wires. Moreover, the probe can eliminate the external disturbances, such as temperature drift, characteristic of the peaks and valleys of the wire rope. The detection sensitivity of the broken wires can be improved.

III. EDDY CURRENT TESTING SIMULATION OF THE BROKEN WIRE

A. GOVERNING EQUATIONS BASED ON A_r, V-A_r

Based on the $\boldsymbol{A}_r$, $V-\boldsymbol{A}_r$ formulations, the governing equations of the finite element model for ECT of the steel wire rope is as follows:

$$-\frac{1}{\mu_0}\nabla^2\boldsymbol{A}_r + j\omega\sigma\left(\boldsymbol{A}_r + \nabla v\right) = -\nabla\times\boldsymbol{H}_s - j\omega\sigma\boldsymbol{A}_s\,(\Omega_1) \tag{1}$$

$$\nabla\cdot\left(-j\omega\sigma\boldsymbol{A}_r - j\omega\sigma\nabla v\right) = \nabla\cdot j\omega\sigma\boldsymbol{A}_s\,(\Omega_1) \tag{2}$$

$$-\frac{1}{\mu_0}\nabla^2\boldsymbol{A}_r = 0\,(\Omega_2) \tag{3}$$

where $\boldsymbol{A_r}$ stands for the simplified magnetic vector potential. In Eqs. (1) and (2), $\upsilon = V/(j\omega)$. V represents the simplified electrical scalar position. The domain of the steel wire rope model (Ω_1) and the domain of the air with the power supply (Ω_2) constitute the entire solution domain. In Eqs. (1)-(3), $\boldsymbol{A}_s$ and $\boldsymbol{H}_s$ represent the magnetic vector position and magnetic field strength generated by the excitation current in the solution domain, respectively. μ_0 represents the magnetic permeability of the air. ω stands for the angular frequency of the current source. When the potential solution is obtained, the EC density can be calculated according to Eq. (4):

$$\boldsymbol{J} = -j\omega\sigma\left(\boldsymbol{A} + \nabla v\right) \tag{4}$$

where $\boldsymbol{A}$ is the vector sum of $\boldsymbol{A}_s$ and $\boldsymbol{A}_r$.

B. THE SIMULATION MODEL

Fig.3 is the simulation model containing the steel wire rope and the EC differential probe. The rope is a 6 × 19 ordinary lay wire rope. Its total length is 240 mm. The lay length is 60 mm. Its conductivity is 3.0×10^7S/m and the relative magnetic permeability is 10 [19]. Two EC differential probes are designed. The size of the four pancake coils is the same. The coil has an inner diameter 4.0 mm, an outer diameter 7.0 mm, a height 2.0 mm, a number of turns 500, and a lift-off 1 mm. Coil a_1 and coil a_2, coil b_1 and coil b_2 are symmetric about the axis of the rope, respectively. The excitation current is 80 kHz and the magnitude is 1 A.

EC mainly concentrates on the surface of the rope due to the skin effect. Hence the surface broken wires are prone to

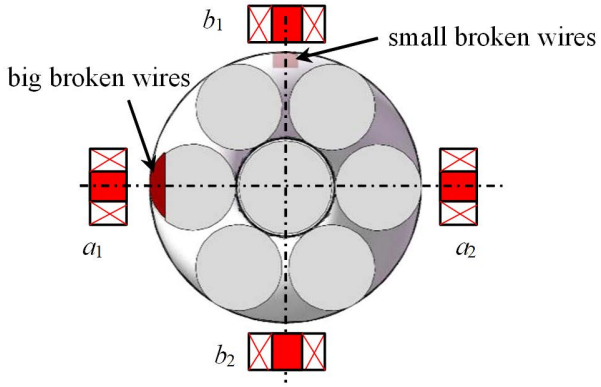

FIGURE 3. The simulation model containing the steel wire rope and the EC differential probe.

be detected. In this section two degrees of defect are made, named small broken wires and big broken wires, respectively. The small broken wires are just under the coil b_1 and are located at $z = 15$ mm. The big broken wires are just under the coil a_1 and are located at $z = -10$mm. The simulation model is then meshed automatically. The finite element analysis is then established.

C. SIMULATION RESULTS OF SCANNING THE BROKEN WIRES

Fig.4 is the scanning results of the broken wires obtained by the finite element analysis. The abscissa is the scanning position of the EC differential probe. The ordinate is the real part of the output voltage of the EC differential probe.

The red solid line donates the variation of the differential voltage between the coil a_1 and the coil a_2 with the scanning position. The big broken wires at $z = -10$ mm make the signal significantly increased. The distribution of EC is disturbed by the big broken wires just under the coil a_1. Hence the output voltage of the EC differential probe is not zero. When the coil a_1 and the coil a_2 scan near the small broken wires at $z = 15$ mm, the signal changes slightly. The distribution of EC is slightly disturbed by the small broken wires just perpendicular to the coil a_1. The black solid line represents the change of the differential voltage between the coil b_1 and the coil b_2 with the scanning position. The signal at $z = 15$ mm changes rapidly due to the small broken wires. When the coil b_1 and the coil b_2 are near the big broken wires at $z = -10$ mm, the real part of the voltage reduces slightly. At $z = -10$ mm, the axes of the coil b_1 and the coil b_2 are perpendicular to the axis of the wire rope. At $z = -10$ mm, the axes of the coil b_1 and the coil b_2 are parallel to the axis of the wire rope. EC induced by the coil b_1 and the coil b_2 is slightly disturbed at $z = -10$ mm compared with the condition at $z = 15$ mm.

In addition, the changes of the output voltage are locally in the shape of "M" from $z = -20$ mm to $z = -0$ and from $z = 10$ mm to $z = 20$ mm. When the axes of the coils are near $z = 15$ mm and $z = -10$ mm respectively, the distribution of EC disturbed by the broken wires is symmetric about the coil axes. When the axes of the coils are near $z = -15$ mm, $z = -5$ mm, $z = 12$ mm, and $z = 18$ mm, the symmetric distribution of EC is disturbed by the broken wires. Hence the output voltage reaches the local maximum.

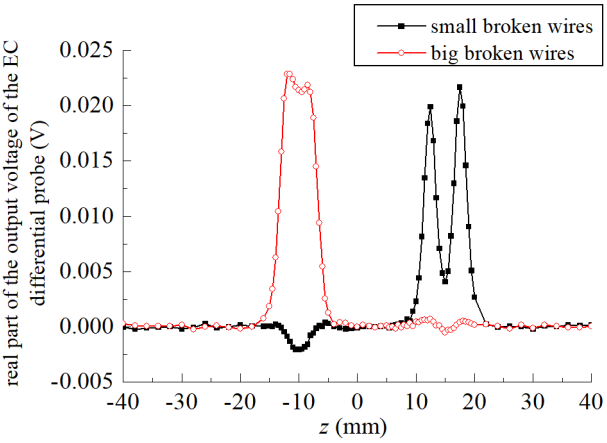

FIGURE 4. The simulated output voltage of the EC differential probe scanning the broken wires with two different degrees.

IV. EXPERIMENTAL VERIFICATION

A. EXPERIMENTAL PLATFORM

An experimental platform is built for detecting the broken wires, as shown in Fig.5. A signal generator (RIGOL DG4102) provides the exciting signal with a frequency of 80 kHz and an amplitude of 10V. An electronically controlled displacement platform is assembled to realize the straight-line movement of the probe. The wire rope is scanned at a step of 1 mm. The RF Lock-In Amplifier (SR844) receives the voltage signal and the data is acquired and displayed via LABVIEW.

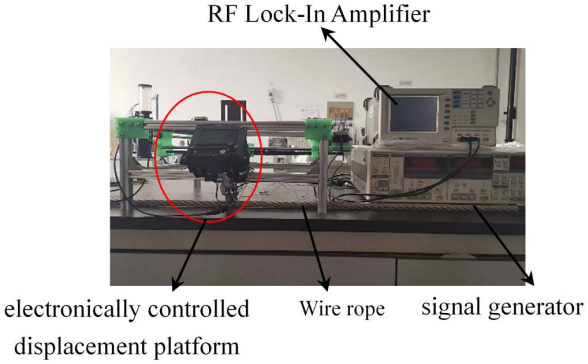

FIGURE 5. The eddy current testing experimental platform for detecting the surface broken wires.

Fig. 6 is the steel wire rope sample. The length is about 1 m and the lay length is 60 mm. The diameter of the rope is about 10 mm. The sample is designated by 6×19 OL and OL means ordinary lay. There are three manually made defects on the sample, labeled as point a, point b, and point c. At point a multiple broken wires are grinded by a file and smaller broken

wires are grinded at point *b*. Point *a* and point *b* are on the peaks of the surface. In order to verify the detect ability of the eddy current testing, the broken wires with the same defect degree of point *a* are grinded on the valleys of the surface at point *c*.

Fig. 7 shows the proposed EC differential probe. The broken wires in Fig. 6 are in the same side of the rope, so the probe is assembled by two pancake coils with the same size, denoted by coil 1 and coil 2, respectively. This is the reason that the coil in experiment is different from the coil in simulation shown in Fig. 2 and Fig. 3. In Fig. 7 the coils are put in a plastic support frame and the frame is printed by a 3D printer. Coil 1, coil 2, and the DC resistances form a differential circuit printed on a PCB board. Coil 1 and coil 2 have an inner diameter 4 mm, an outer diameter 7 mm, a height 2 mm, and a number of turn 240. Both the DC resistance 1 and 2 are 100 Ω.

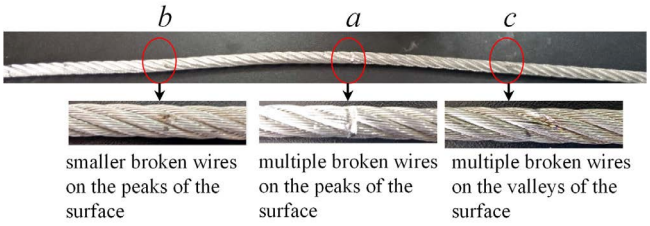

FIGURE 6. The steel wire rope sample with different degrees of broken wires.

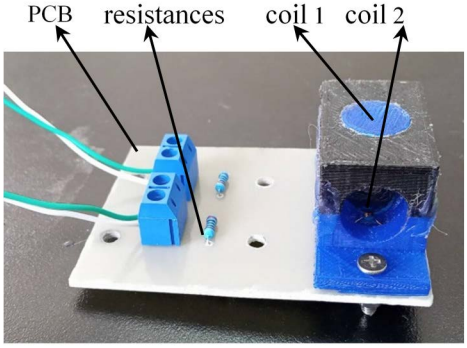

FIGURE 7. The proposed EC differential probe.

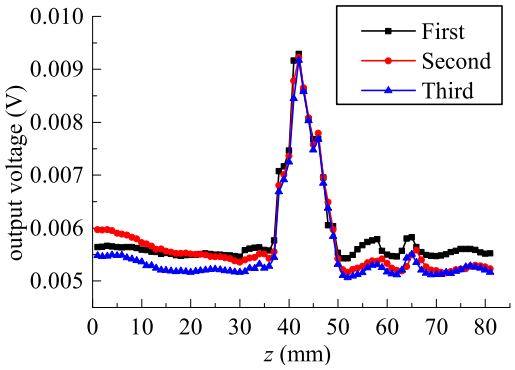

(a) scanning the multiple broken wires on the peaks of the surface labeled as point *a*

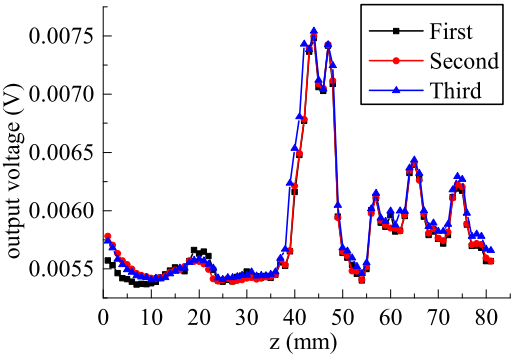

(b) scanning the smaller broken wires on the peaks of the surface labeled as point *b*

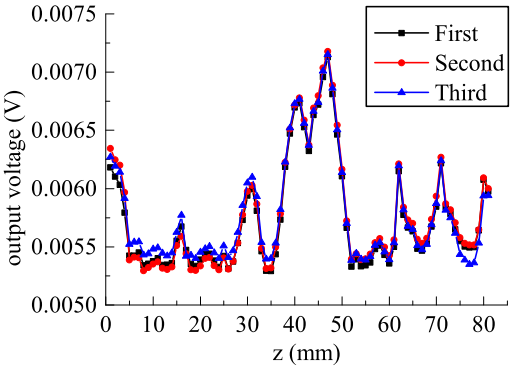

(c) scanning the multiple broken wires on the valleys of the surface labeled as point *c*

FIGURE 8. The scanning results of different degrees of surface broken wires in Fig. 6.

B. EXPERIMENTAL RESULTS

To ensure the validity of detecting the broken wires, each defect is scanned three times with interval of 10 minutes. The defect is in the middle of the scanning range and the scanning length of each defect is 80 mm. Fig. 8 shows the scanning results of the broken wires. The abscissa is the scanning position of the eddy current differential probe. The ordinate is the amplitude of the output voltage of the eddy current differential probe. The detection results of different degrees of broken wires in Fig. 6 are depicted in Fig. 8 (a)-(c), respectively. The three times scanning results of the broken wire have the same trend. In Fig. 8 (a), when the probe is far away from the defect, the voltage amplitude appears small fluctuation. The reason is that the coils can not be kept the same and symmetrical about the axis of the rope during the making process and the rope sample is not straight during the scanning process. The voltage amplitude increases dramatically as the probe is near the broken wires ($z = 40$ mm). The eddy current is disturbed by the multiple broken wires at point *a*, therefore the eddy current under the two coils are no longer symmetrical. The "M" shape characteristic in Fig. 4 is not obvious in Fig. 8. In experiment the output voltage is contaminated by the electromagnetic interference in the environment and the ratio of signal to noise (S/N) is greatly reduced.

The defect degree at point *b* is weaker than that at point *a*, so the variation of the output voltage with the scanning position is more obvious in Fig. 8 (a). Meanwhile defect at point *c* is at the valleys, so the disturbance of the eddy current at point *c* is weaker than that at point *a*.

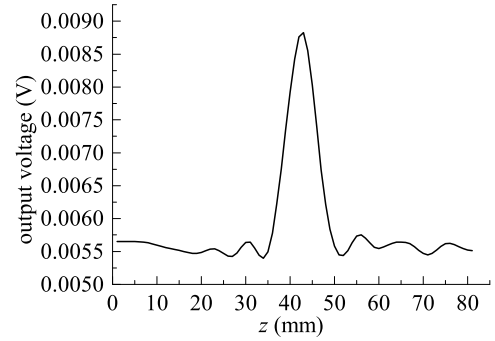

(a) post processed result of signal in Fig. 8 (a)

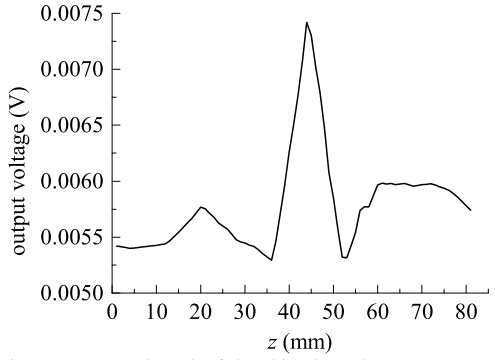

(b) post processed result of signal in Fig. 8 (b)

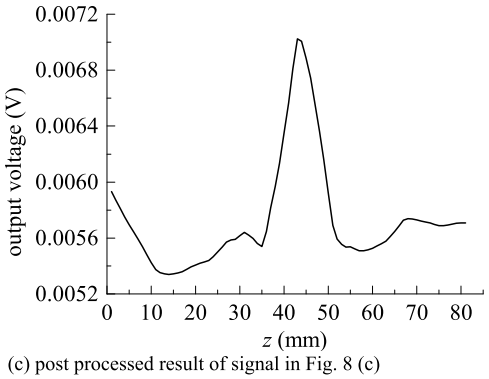

(c) post processed result of signal in Fig. 8 (c)

FIGURE 9. The post processed results of the original signal in Fig. 8 by wavelet transform.

C. POST PROCESSING OF THE EXPERIMENTAL RESULTS

In order to improve S/N in Fig. 8, the eddy current response signal is post processed. Wavelet transform has good time-frequency localization characteristics. The wavelet coefficients of signal and noise have different properties in each scale, so it can be used to reduce the noise of non-stationary signals.

By selecting the appropriate threshold, the wavelet coefficients formed by the wavelet transform are processed by the soft threshold method. Then the signal is reconstructed. The post processed results of the original signal in Fig. 8 are shown in Fig. 9. Compared with the results in Fig. 8, the output voltage in Fig. 9 changes smoothly on the intact region of the sample. The signal change due to the broken wires is more obvious.

To quantitatively compare the detection sensitivities of the broken wires, a parameter named the change ratio of the output voltage is defined as the relative change ratio of the output voltage at the intact region and the broken wires. Table 1 lists the change ratio of the output voltage at point *a*, point *b*, and point *c*. The output voltage at the intact region is the average value of the intact region in Fig. 9 (a)-(c), respectively. The output voltage at point *a*, point *b*, and point *c* is the maximum of Fig. 9 (a)-(c), respectively. In Table 1, the change rate of the output voltage is 58.06%, 37.15%, and 26.94% at point *a*, point *b*, and point *c*, respectively. When the broken wires are more serious on the peaks of the rope surface, the change rate of the output voltage is larger. When the broken wires are on the valleys of the rope surface, the detection sensitivity is reduced.

TABLE 1. Quantitative analysis of the detection of the surface broken wires.

Position of the broken wires	Voltage at the intact region	Voltage at the broken wires	The change rate of the output voltage
Point *a*	5.58 mV	8.82 mV	58.06%
Point *b*	5.41 mV	7.42 mV	37.15%
Point *c*	5.53 mV	7.02 mV	26.94%

V. CONCLUSION

The eddy current detection method of the surface broken wires of the steel wire rope is researched in this study. The EC differential probe is designed according to the spiral structure of the rope. The following conclusions are obtained:

(1) The designed EC differential probe can be used to eliminate the influence of the surface alternating peaks and valleys of the rope on the EC signal of the broken wires. The simulated real part of the output voltage of the EC differential probe changes in ''M'' shape.

(2) The relative change ratio of the output voltage increases with the degree of the surface broken wires. In the future work, a physical feature named the relative change ratio of the ouput voltage will be used in the inverse solution of the degree of the surface broken wires.

ACKNOWLEDGMENT

The authors would like to thank the valuable help of their coworkers.

REFERENCES

[1] J. Tian, J. Zhou, H. Wang, and G. Meng, "Literature review of research on the technology of wire rope nondestructive inspection in China and abroad," in *Proc. Int. Conf. Eng. Technol. Appl.*, Xiamen, China, 2015, Art. no. 03025.

[2] Z. Jijun and M. Xiangqing, "Defect detection of wire rope for oil well based on adaptive angle," *Frattura ed Integrità Strutturale*, vol. 34, pp. 590–598, Sep. 2015.

[3] R. Schlanbusch, E. Oland, and E. Bechhoefer, "Condition monitoring technologies for steel wire ropes—A review," *Int. J. Prognostics Health Manage.*, vol. 8, no. 1, pp. 1–14, 2017.

[4] P.-C. Peng and C.-Y. Wang, "Use of gamma rays in the inspection of steel wire ropes in suspension bridges," *NDT E Int.*, vol. 75, pp. 80–86, Oct. 2015.

[5] J. Zhang, X. Tan, and P. Zheng, "Discontinuities from residual magnetic field images using Hilbert–Huang transform and compressed sensing," *Sensors*, vol. 17, no. 3, pp. 1–19, 2017.

[6] J. H. Kurz, L. Laguerre, F. Niese, L. Gaillet, K. Szielasko, R. Tschuncky, and F. Treyssede, "NDT for need based maintenance of bridge cables, ropes and pre-stressed elements," *J. Civil Struct. Health Monitor.*, vol. 3, no. 4, pp. 285–295, Dec. 2013.

[7] J. Wu, H. Fang, X. Huang, H. Xia, Y. Kang, and C. Tang, "An online MFL sensing method for steel pipe based on the magnetic guiding effect," *Sensors*, vol. 17, no. 12, p. 2911, 2017.

[8] S. Wu, "Experimental research on signal characteristics of broken Wires in wire rope," M.S. thesis, Dept. Saf. Sci. Eng., Jiangxi Univ. Sci. Technol., Jiangxi, China, 2015.

[9] L. Collini and F. Degasperi, "MRT detection of fretting fatigue cracks in a cableway locked coil rope," *Case Stud. Nondestruct. Test. Eval.*, vol. 2, pp. 64–70, Oct. 2014.

[10] D. Slesarev, K. Myakushev, and I. Shpakov, "Specific aspects of inspection of large diameter steel ropes," in *Proc. OIPEEC Conf.*, Hague, The Netherlands, 2019.

[11] S. Yang and Y. Kang, *Quantitative Detection Principle and Technology of Broken Wire of Steel Wire Rope*. Arlington, TX, USA: National Defense Industry Press, 1995, pp. 62–114.

[12] W. Bai, M. Chai, L. Li, Y. Li, and Q. Duan, "Acoustic emission from elevator wire rope during tensile testing," in *Proc. World Conf. Acoustic Emission*, Shanghai, China, 2013, pp. 217–224.

[13] R. Raišutis, R. Kažys, L. Mažeika, E. Žukauskas, V. Samaitis, and A. Jankauskas, "Ultrasonic guided wave-based testing technique for inspection of multi-wire rope structures," *NDT E Int.*, vol. 62, pp. 40–49, Mar. 2014.

[14] D. A. Hill and J. R. Wait, "Electromagnetic field perturbation by an internal void in a conducting cylinder excited by a wire loop," *Appl. Phys.*, vol. 18, no. 2, pp. 141–147, Feb. 1979.

[15] S. Hiruma and H. Igarashi, "Fast three-dimensional analysis of eddy currents in Litz wire using integral equation," in *Proc. IEEE Conf. Electromagn. Field Comput. (CEFC)*, Nov. 2016, p. 1.

[16] Q. Cao, D. Liu, Y. He, J. Zhou, and J. Codrington, "Nondestructive and quantitative evaluation of wire rope based on radial basis function neural network using eddy current inspection," *NDT E Int.*, vol. 46, pp. 7–13, Mar. 2012.

[17] V. Sukhorukov, "Steel-cored conveyor belt NDT," in *Proc. Int. Conf. Slovenian Soc. Non-Destructive Testing*, 2005.

[18] T. Li, Z. Zeng, and J. Wu, "Analysis of eddy current response to lay length of wire rope with pancake coil and experimental study," *J. Mech. Eng.*, vol. 56, no. 16, pp. 13–21, 2020.

[19] F. Fu, "Design of three-phase asynchronous motor," in *Design Manual of Asynchronous Motor*. Beijing, China: China Machine Press, 2003.

KOU YANFEI was born in Shaanxi, China, in 1984. He received the Eng.D. degree from the Taiyuan University of Technology, in 2016. He is currently an Associate Professor with the North University of China. He is also a Tutor for graduate graduates. He has presided over more than ten major province science and technology projects, including the Natural Science Foundation of Shanxi Province and the Science and Technology Research Plan Project of Shaanxi Province. He participated in the National Science and Technology Project of China. His research interests include electro-hydraulic equipment monitoring and control and testing instruments.

GUO JIUJIANG was born in Shanxi, China, in 1994. He received the B.S. degree in vehicle engineering from the Shanxi Jinzhong Institute of Technology, in 2018. He is currently pursuing the degree in mechanical engineering with the School of Mechanical Engineering, North University of China. His research interests include non-destructive testing and special equipment inspection.

LI JINGJING was born in Shanxi, China, in 1997. She received the bachelor's degree in electrical engineering and automation from the Shanxi Institute of Energy, in 2019. She is currently pursuing the degree in industrial engineering and management with the School of Mechanical Engineering, North University of China. Her current research interests include the design of test systems and non-destructive testing.

JIAO SHAONI was born in Shanxi, China, in 1986. She received the Eng.D. degree from the Xiamen University of Technology, in 2017. She is currently a Lecturer with the Taiyuan University of Technology. She had participated in the National Science and Technology Project of China and the Natural Science Foundation of Xiamen Province. Her research interests include numerical simulation and eddy current testing.

LIU JIQUAN was born in Chongqing, China, in 1980. He received the master's degree from the College of Mechatronics Engineering, North University of China. He is currently an Associate Researcher with the Tai Yuan Research Institute of China Coal Technology & Engineering Group. He has presided over or participated in more than 40 major science and technology projects. His research interests include power machinery and mining machinery and testing instruments.

YAN ZHIWEI was born in Taiyuan, China, in 1978. He received the master's degree from Yanshan University. He is currently a Senior Engineer with the Tai Yuan Research Institute of China Coal Technology & Engineering Group. He has presided over or participated in more than 50 major science and technology projects. His research interests include mining machinery and testing instruments.

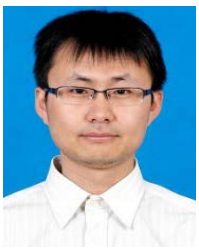

ZHU KUN was born in Wenzhou, China, in 1985. He received the master's degree from the China University of Mining & Technology, Beijing. He is currently an Assistant Research Fellow with the China Coal Research Institute. He has presided over or participated in more than 20 major science and technology projects, including the Scientific Research Project of the China Coal Technology & Engineering Group and the National Natural Science Foundation of China. His research interests include coal mining and project management.